Volume 17, Issue 2, 172511 (1-6)

Iranian Journal of Earth Science (IJES)

https://doi.org/10.57647/j.ijes.2025.1702.11

Investigating the effectiveness of frequency measurement methods for spin echo enhanced proton precession magnetometers

Yasamin Elmi Ghiasi[1], Faeze Mahboubian[1], Hadi Sharifi Tameh[2], Farrokh Sarreshtedari[1,*]

[1]*Quantum Resonance Research Laboratory, Department of Physics, College of Science, University of Tehran, Tehran, Iran.*
[2]*School of Electronics, Electrical Engineering and Computer Science, Queen's University Belfast, Belfast, UK.*

[*]**Corresponding author:** f.sarreshtedari@ut.ac.ir

Original Research

Received:
13 March 2024
Revised:
10 June 2024
Accepted:
3 November 2024
Published online:
10 April 2025

Abstract:

The incorporating frequency measurement technique has a very important role in the determination of achievable sensitivity using NMR-based magnetometers for earth field measurements. This is while, the selection of the frequency calculation algorithm, determines the required resources of the digital processing hardware for such magnetometers. We have previously developed a proton precession magnetometer equipped with a spin echo mechanism that could measure the gradient of the magnetic field as well as the magnitude of the magnetic field. In this magnetometer, a switching field is used for making the spin echo which decreases the effective spin-spin relaxation time constant. The reduction of this time constant increase the decay rate of the NMR signal and so the frequency calculation for obtaining the Larmor frequency should be accomplished in a shorter time. In this work, different frequency calculation methods are investigated for achieving high-sensitivity earth field measurements. In this regard, both time domain and frequency domain analysis of free induction decay (FID) frequency calculation is implemented and compared. The effect of SNR and decay time constant of FID signal on the accuracy of Larmor frequency calculation is discussed. It is shown that frequency domain analysis is much preferred for frequency calculation especially when using the spin echo enhanced proton precession magnetometer.

Keywords: Spin echo enhanced proton precession magnetometer; Nuclear magnetic resonance; Larmor frequency; Frequency measurement techniques

1. Introduction

The physics of proton precession magnetometer is based on nuclear magnetic resonance phenomena (Chizhik et al., 2014). The operation of these magnetometers has two steps. In the first step, protons of the system get spin polarized by applying an appropriate magnetic field. In the second step, the polarized protons precess around the environment magnetic field with Larmor frequency (Ripka, 2001; Mahboubian et al., 2019). The NMR precessing protons induce a damping sinusoidal signal on the detection coils, which have the same frequency. This signal, known as the free induction decay (FID) signal, can be approximated as equation (1):

$$y = \sin(2\pi f t + \frac{\pi}{2}) \times e^{(-\lambda t)} + \text{noise} \qquad (1)$$

In this equation, f is the frequency that we want to measure and λ is the decay constant which is proportional to the inverse of T2* (Ripka, 2001). Measuring the frequency f, the environment magnetic field could be found using the NMR relation, which is shown in equation (2):

$$\omega = \gamma B \qquad (2)$$

where γ is the gyromagnetic ratio constant and B is the environment magnetic field. Using equation (2), for achieving a typical 1nT accuracy, we should measure the frequency at least with 0.05 Hz accuracy. The precession signal is read at a specified time interval, which is typically around a few seconds in low measurement rate magnetometers. The signal amplitude decreases during this interval, depending on the decay constant (λ). Two of the important parameters

that affect the accuracy of the NMR frequency are the measurement interval and signal-to-noise ratio of the obtained signal. Different works are devoted to noise cancellation and analysis of the proton precession FID signal (Yazdi et al., 2016; Liu et al., 2017; Dong et al., 2016; Tan et al., 2019; Liu et al., 2020). In reference (Sarreshtedari et al., 2020), we have introduced Gradient spin echo enhanced proton precession magnetometers, which measure the field gradient in addition to the magnetic field. In this system, a switching gradient field applies during field measurement which reduces the effective spin-spin relaxation time constant ($T2^*$) and increases the decay rate. Therefore, it is important to incorporate appropriate frequency calculation techniques for efficient measurement of the magnetic field and magnetic field gradient.

The NMR frequency measurement could be performed both in time and frequency domains. The type of the frequency measurement technique has a great impact on the selection of the required platform for hardware implementation of the system. In fact, for a field operational magnetometer, the real-time Larmor frequency calculation should be performed in a digital platform like a high-performance microcontroller, field programmable gate array (FPGA), DSP processor, or other similar devices. Each of these parts has its own advantages and disadvantages in terms of available processing resources, implementation complexity, power consumption, price, etc. This is while, the processing capability for the implementation of the frequency calculation algorithm (either in time domain or frequency domain) is the main criteria for selecting the appropriate processing platform. In this regard, considering the relative simplicity of the implementation of the Larmor frequency calculation in time domain, we have tried to determine the maximum accuracy that can be achieved by this method. In this work after a brief explanation of different frequency measurement methods and our experimental setup, we have investigated the result of applying the time and frequency domain methods to NMR signals with different decay constant rates.

2. Frequency calculation of NMR signal in time and frequency domains

There are two conventional time-domain frequency measurement methods. One of them is based on counting the number of signal cycles in a specific time interval. This approach is appropriate for relatively high frequency signals, which have many cycles in the measurement interval. As the NMR signal of the proton precession magnetometer has a low Larmor frequency of about 2 KHz for the earth's magnetic field, this method is not appropriate and is not considered here. The second time-domain frequency measurement method, called the period approach, is based on using a much higher auxiliary signal and counting its cycles that take place in a period of the unknown signal. By counting the number of rising (or falling) edges of the auxiliary signal in each period of the NMR signal, the Larmor frequency is obtained according to equation (3):

$$F_{\text{Larmor}} = \frac{1}{N \times T_{aux}} = \frac{F_{aux}}{N} \tag{3}$$

where N is the number of counts, T_{aux} is the period of auxiliary signal and so F_{aux} is the frequency of auxiliary signal. Here the auxiliary frequency is as the same as the sampling frequency of the data acquisition system. Furthermore, as we just require calculating the frequency, after data acquisition, a signal-conditioning step is considered so that each positive data is assigned a value of 1 and otherwise 0. Because of the added noise to the signal, where the amplitude of the sinusoidal signal is close to zero, signal recognition is associated with the error, which results in an error in frequency calculation. The larger the signal-to-noise ratio, the lower the error data. In addition, since the amplitude of the signal decreases with the λ; over time, its value becomes significant compared to the noise. Therefore, after a considerable decaying of the amplitude, the signal-to-noise ratio (SNR) decreases and so the error data increases significantly. In this regard, a cutting point is considered in such a way that the frequency is measured and averaged in an interval from the beginning of the signal to this specific point. In frequency measurement, the largest error is due to end-of-interval data, so although cutting the signal reduces the averaging number but appropriate cutting results in error reduction. For further noise cancelation, a threshold frequency is defined where the frequencies greater than that are removed from the averaging. In addition, we have also used a convolution filtering method based on a moving average box (Oppenheim and Schafer, 2009). In this method, $y(t)$, in equation (1), is modified by function $g(t)$ where defined as equation (4):

$$g(t) = \begin{cases} \frac{1}{L}, & \text{if } t \in [0, L] \\ 0, & \text{otherwise.} \end{cases} \tag{4}$$

And the smoothed $y(t)$ is obtained according to equation (5).

$$y_{\text{smooth}} = (y * g)(t) = \int_{-\infty}^{+\infty} f(T)g(t-T)dT \tag{5}$$

In this approach, by changing the L in the $g(t)$ function, y_{smooth} finds a different resolution. Using equation (5), the noise of the signal could be efficiently eliminated and as a result, the error in frequency measurement would be reduced. Figure 1 shows a part of a sample input signal and its smoothed counterpart.

It should be noted that, $g(t)$ is a rectangular window in time domain which has a frequency response of $\text{sinc}(\omega L)$. In this

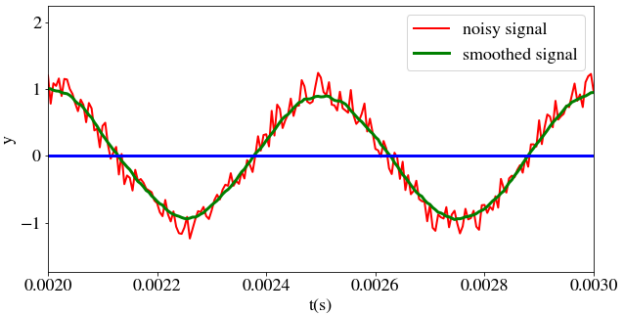

Figure 1. A sample input signal and its smoothed counterpart. Smoothing is done by convolution method ($L = 20$).

regard $g(t)$ could be considered as a frequency filter with a bandwidth proportional to $1/L$. The frequency response of the convolution (equation (5)), results in multiplication of the spectrum of the NMR signal and the mentioned sinc type function. It should be noted that, the sinc filter has a main lobe with the mentioned bandwidth and also many side lobes. So, it is not an ideal frequency filter compared to the rectangular frequency filters. It is also worth emphasizing that, the implementation of this time domain noise cancellation method does not need obtaining the frequency content of the NMR signal. Besides the mentioned time domain analysis, frequency domain calculation of proton precession Larmor frequency is based on a well-known fast Fourier transform (FFT) (Oppenheim and Schafer, 2009). FFT converts the digital signal from its time domain to frequency domain by decomposing a sequence of values into components of different frequencies (Heideman et al., 1984). The sampling rate of the measurement and the selected number of samples (block length) are the two central parameters of an FFT which according to equation (6), determine the frequency resolution.

$$df = \frac{fs}{BL} \tag{6}$$

where df is the frequency resolution which determines the frequency spacing between two measurement results. fs is the sampling rate and BL is the block length which is an integer power to the base 2 (Oppenheim and Schafer, 2009). Fig. 2 shows the frequency spectrum (FFT) of a measured NMR signal using spin echo enhanced proton precession magnetometer. Using the FFT spectrum of FID signal, the Larmor frequency could be obtained by finding the maximum peak of the spectrum.

It is worth mentioning that, there is an inverse relationship between the time duration of the FID signal and the width of the frequency spectrum. The shorter the duration of the FID signal (high decay rate), the wider the peak in the FFT spectrum which reduce the precision of the Larmor frequency extraction. In the next section, we explain the experimental setup for obtaining the proton precession signal with different damping constants, and in section 4, the comparison of the calculation methods (in time and frequency domains) for achieving the Larmor frequency is discussed.

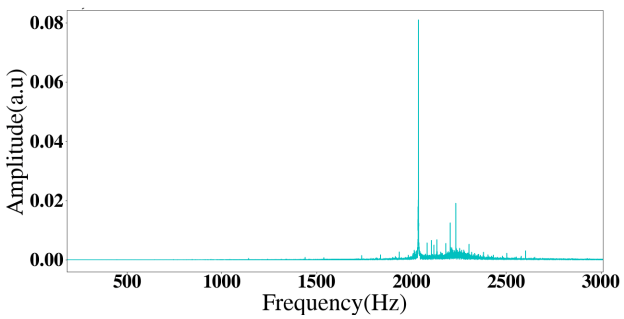

Figure 2. The frequency spectrum of a measured NMR signal using spin echo enhanced proton precession magnetometer. The sampling rate is 200 KHz.

3. Experimental setup

Figure 3 shows the experimental setup of the spin echo enhanced proton precession magnetometer (Sarreshtedari et al., 2020). This system is composed of a proton precession magnetometer with modified polarization and detection process control, and a set of Maxwell coils for applying a switching gradient field. The sensor is a cylindrical reservoir with a diameter of 8 cm and a height of 13 cm containing a solution of water and alcohol which is a hydrogen rich liquid. Protons are polarized with a current of about 1 A using a polarizing coil that is wound around this reservoir. The mentioned coil also acts as the detection coil after the polarization time. This sensor is placed in the middle of a large Maxwell coil for applying magnetic field with a constant gradient. We have incorporated this system for obtaining FID signals with different decay rates. The lower the gradient of the ambient field, the lower the attenuation constant, and the obtained precession signal slowly decays. These signals are used for characterizing the frequency measurement techniques. It should be noted that we have used the computer sound card as the data acquisition part of the system which converts the analog output signal of the magnetometer to a digital signal by a sampling rate of 200 kHz. The analog amplifier has a voltage gain of about 105 and a bandwidth of a few hundred hertz around 2 kHz center frequency which corresponds to the Larmor frequency of typical earth magnetic fields. This bandpass filter of the analog amplifier effectively eliminates the sensor induced noise which its frequency content is out of the mentioned narrow bandwidth. Furthermore, the 200 kHz sampling rate is sufficiently (about 100 times) greater than Larmor frequency (about 2 kHz) which guarantees the appropriate data conversion. The resulting digitized data is then used for digital frequency measurement.

Figure 4 shows a typical FID signal of this magnetometer system. This signal, which is obtained without applying a gradient field, is used here as the reference in frequency calculation analysis. It is evident that the time interval of the measured precession signal is 5 seconds.

Figure 3. The experimental setup of the spin echo enhanced proton precession magnetometer.

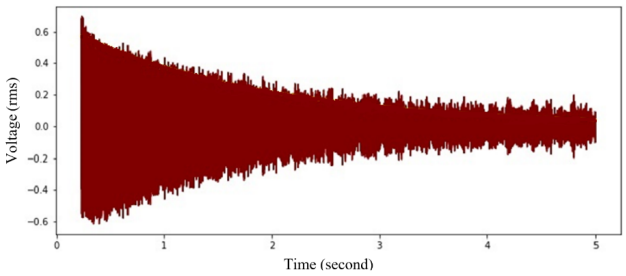

Figure 4. A free induction decay (FID) signal of the spin echo enhanced proton precession magnetometer.

4. Results and discussion

For investigating the effectiveness of different frequency calculation methods, we have incorporated both the simulated precession signals as well as experimentally obtained signals. The Larmor frequency has been calculated by the mentioned methods for signals with different SNR and λ. Figures 5-7 show the result of the frequency calculation of the simulated NMR signal using the period method in terms of signal-to-noise ratios. The simulated signal is produced using equation (1) and different signal enhancements are compared. The frequency is set to $f = 2$ kHz, the SNR is changed from 5 to 100 and different decay constants are considered.

Figure 5 shows the effect of calculation time interval selection for the case of $\lambda = 1$. It is evident that if the whole three seconds of the signal is used for frequency calculation, the results are unacceptable except for very high signal-to-noise ratios.

Figure 6 shows the effect of the input signal decay constant on the result of time-domain frequency calculation in terms of SNR. As expected, the result is more acceptable for lower decay constant especially in low SNR values. Here the frequency interval of $\min(f) < f_{\text{acceptable}} < \max(f)/2$ is considered for keeping the acceptable frequency results in averaging. Using such a filtering threshold considerably improves the averaging accuracy by removing the out-of-range values. The results of using the convolution method for signal smoothing and decreasing the calculated frequency error are shown in figure 7. For comparing different $g(t)$ functions, according to equation (4), three different values of L are considered and the frequencies for the decay constant of $\lambda = 1$ are represented. As can be seen, the smaller L in the $g(t)$ function, the better the frequency accuracy. Incorporation of this smoothing method considerably improves the calculation accuracy in such a way that the obtained results are near to the desired accuracy of 0.05 Hz for signals with SNR greater than 10 and decay constant less than 0.5.

In contrast to time-domain frequency calculation, obtaining the Larmor frequency in the frequency domain has a much lower dependence on decay rate and signal-to-noise ratio. In this approach, obtaining the discrete Fourier transform of the input signal, the maximum peak gives the Larmor frequency. The most important parameter that determines the accuracy of the obtained frequency is the sampling rate, which in our case is fixed and equal to 200 kHz. Figure 8 shows the experimental FID signals obtained by applying different gradient fields, which results in different decay rates. It should be noted that the applied gradient field does not change the Larmor frequency but by decreasing the $T2^*$, result in decreasing the decay rate of the FID signal. The added solid curves in these figures are the fitted exponential for obtaining the decay constant. The calculated decay constant for signals (a)-(d) are 0.63, 0.94, 1.07, and 7.31 respectively.

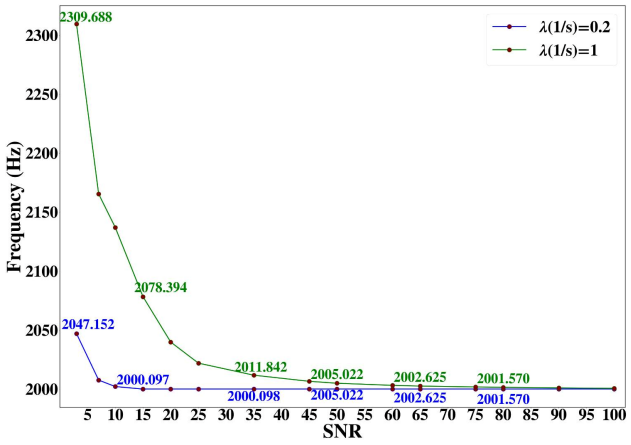

Figure 6. The frequency calculation result for two signal decay constants in terms of SNR.

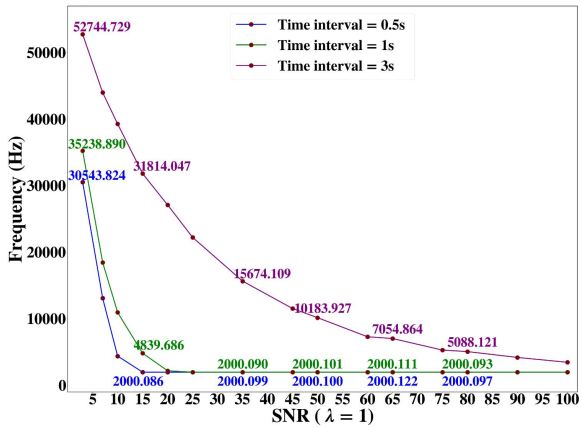

Figure 5. The frequency calculation result for selecting time intervals of 0.5, 1 and 3 seconds.

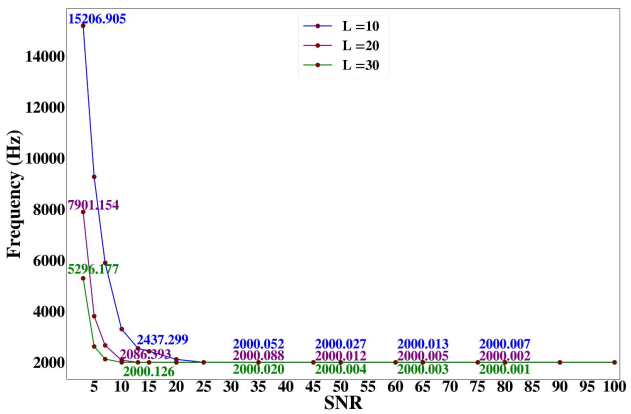

Figure 7. The results of using convolution method with three different L values (10, 20 and 30) of $g(t)$ function.

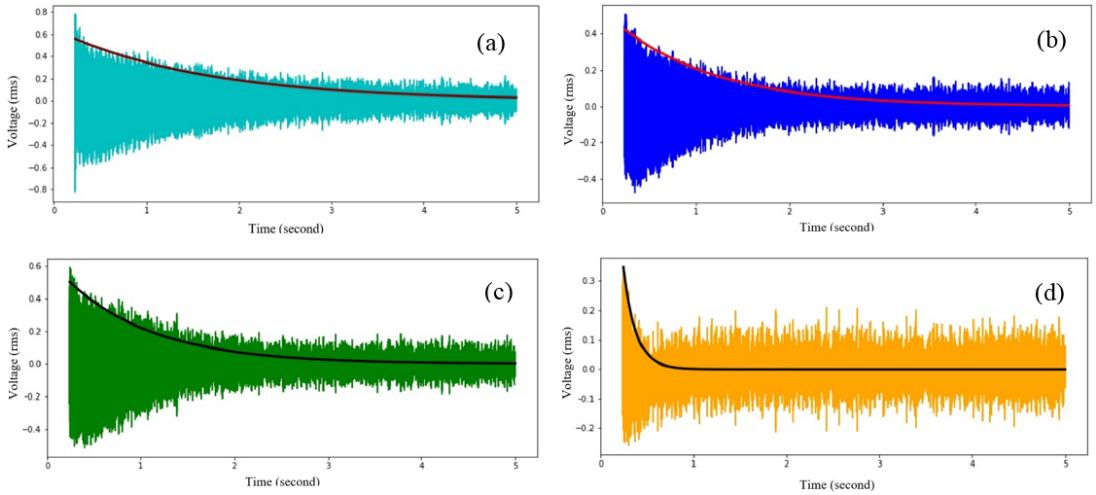

Figure 8. The experimental results of FID signals with different decay rates. (a) $\lambda = 0.63$, (b) $\lambda = 0.94$, (c) $\lambda = 1.07$, (d) $\lambda = 7.31$.

The Larmor frequency of the signals shown in figure 8 is calculated using time-domain and frequency-domain methods. In the time-domain method, all mentioned signal enhancement techniques like convolution-based smoothing and averaging in the appropriate time interval are used. It is observed that although the time-domain method with mentioned enhancement, calculates the Larmor frequency with desired accuracy but the result of this method substantially depends to signal decay rate. This is while the frequency-domain method is both accurate and has low dependence on the decay rate. For example, the frequency calculation result of the FID signal shown in figure 8 (c) has just a 0.07% difference from the frequency calculation result of the reference signal (figure 4) with about half the decay rate. As mentioned in (Sarreshtedari et al., 2020), for obtaining the magnetic field and its gradient by spin echo enhanced proton precession magnetometer we require to apply an additional gradient field, which increases the FID decay rates. In this regard, the current work suggests inclusively incorporating the frequency domain calculation for obtaining the Larmor frequency when using this magnetometer.

5. Conclusion

The frequency measurement method is a key factor in determining the sensitivity of proton precession magnetometers. This is while the operation of spin echo enhanced proton magnetometer which results in FID signals with lower T2* and decreased available averaging interval, demanded a new investigation of frequency calculation techniques. Here we first described the time-domain frequency measurement with signal enhancement as well as frequency-domain measurement. Examining the simulated FID signals with different SNR and decay constants and also experimentally obtained FID signals showed that the time-domain frequency measurement could produce desirable results (accuracy of 0.05 Hz) for signals with SNR greater than 10 and decay constant less than 0.5 but is not applicable in lower signal quality conditions. This is while the DFT method provides the desired accuracy of 0.05 Hz with much lower dependence on SNR and decay constant (λ) which is the required factor to be used for spin echo proton precession magnetometer. The implementation of this frequency measurement technique using a field programmable gate array (FPGA) for this magnetometer would be followed and presented in future work.

Authors contributions
All the authors have participated sufficiently in the intellectual content, conception and design of this work or the analysis and interpretation of the data (when applicable), as well as the writing of the manuscript.

Availability of data and materials
The data that support the findings of this study are available from the corresponding author, upon reasonable request.

Conflict of interests
The authors declare that they have no known competing financial interests or personal relationships that could have appeared to influence the work reported in this paper.

References

Chizhik V. I., Chernyshev Y. S., Donets A. V., Frolov V. V., Komolkin A. V., Shelyapina M. G. (2014) Magnetic resonance and its applications. *Springer,* DOI: https://doi.org/10.1007/978-3-319-05299-1.

Dong H., Liu H., Ge J., Yuan Z., Zhao Z. (2016) A high-precision frequency measurement algorithm for FID signal of proton magnetometer. *IEEE Transactions on Instrumentation and Measurement* 65 (4) DOI: https://doi.org/10.1109/TIM.2016.2516299.

Heideman M. T., Johnson D. H., Burrus C. S. (1984) Gauss and the history of the fast Fourier transform. *IEEE ASSP Magazine* 1 (4): 14–21. DOI: https://doi.org/10.1109/MASSP.1984.1162257.

Liu H., Dong H., Liu Z., Ge J., Bai B., Zhang C. (2017) Noise characterization for the FID signal from proton precession magnetometer. *Journal of Instrumentation* 12 DOI: https://doi.org/10.1088/1748-0221/12/07/P07019.

Liu H., Wang H., Bin J., Dong H., Ge J., Liu Z., Yuan Z., Zhu J., Luan X. (2020) Efficient noise reduction for the free induction decay signal from a proton precession magnetometer with time-frequency peak filtering. *Review of Scientific Instruments* 91 (4): 045101. DOI: https://doi.org/10.1063/1.5144714.

Mahboubian F., Sardari H., Sadeghi S., Sarreshtedari F. (2019) Design and implementation of a low noise earth field proton precession magnetometer. *27th Iranian Conference on Electrical Engineering (ICEE2019),*
DOI: https://doi.org/10.1109/IranianCEE.2019.8786372.

Oppenheim A. V., Schafer R. W. (2009) Discrete-time signal processing (3rd ed.) *Pearson*

Ripka P. (2001) Magnetic sensors and magnetometer. *Artech House,*
DOI: https://doi.org/10.1088/0957-0233/13/4/707.

Sarreshtedari F., Mahboubian F., Sardari, H. M. (2020) Gradient spin magnetometer: A novel system for field gradient measurement. *Review of Scientific Instruments* 91 (7): 075105.
DOI: https://doi.org/10.1063/5.0011082.

Tan C., Wang J., Li Z. (2019) A frequency measurement method based on optimal multi-average for increasing proton magnetometer measurement precision. *Measurement* 135:418–423.
DOI: https://doi.org/10.1016/j.measurement.2018.10.016.

Yazdi A., ShahHoseini E., Razavi R. (2016) AMS, A method for determining magma flow in Dykes (Case study: Andesite Dyke). *Research Journal of Applied Sciences* 11 (3): 62–67.
DOI: https://doi.org/10.36478/rjasci.2016.62.67.